

ISOMERIZATION OF C5-C7 LINEAR ALKANES OVER WO₃-ZrO₂ UNDER HELIUM ATMOSPHERE

Sugeng Triwahyono^{a,b*}, Aishah Abdul Jalil^{c,d}, Hairul Amiza Azman^a, Che Rozid Mamat^a

^aDepartment of Chemistry, Faculty of Science, Universiti Teknologi Malaysia, 81310 UTM Johor Bahru, Johor, Malaysia

^bIbnu Sina Institute for Fundamental Science Studies, Universiti Teknologi Malaysia, 81310 UTM Johor Bahru, Johor, Malaysia

^cCentre of Hydrogen Energy, Faculty of Chemical Engineering, Universiti Teknologi Malaysia, 81310 UTM Johor Bahru, Johor, Malaysia

^dDepartment of Chemical Engineering, Faculty of Chemical Engineering, Universiti Teknologi Malaysia, 81310 UTM Johor Bahru, Johor, Malaysia

Article history

Received

15 April 2014

Received in revised form

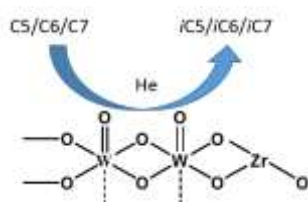
24 December 2014

Accepted

26 January 2015

*Corresponding author
sugeng@utm.my

Graphical abstract



Abstract

The effect of WO₃ on the properties and catalytic isomerization of C5-C7 linear alkanes over ZrO₂ was studied under helium atmosphere. The WO₃-ZrO₂ was prepared by impregnation of Zr(OH)₄ with an aqueous (NH₄)₆[H₂W₁₂O₄₀], followed by calcination at 1093 K for 3 h in air. The amount WO₃ was 10 wt%. XRD and BET studies showed that the introduction of WO₃ stabilizes the tetragonal phase of ZrO₂, leading to larger surface area and stronger acidity of ZrO₂. Pyridine FTIR study verified the interaction of WO₃ with ZrO₂ formed strong Lewis and Bronsted acid sites. The presence of WO₃ increased the catalytic isomerization of C5-C7 linear alkanes. The conversion of C5, C6 and C7 reached 1.3, 2.6 and 5.1 %, respectively. While the selectivity of isopentane, isohexane and isoheptane reached 15.6, 20.5 and 19.5 %, respectively. The high activity of WO₃-ZrO₂ was due to the ability of WO₃ to adsorb and dissociate linear alkane to form hydrogen and alkane radical in which the atomic hydrogen underwent to the formation of protonic acid sites and hydride. The presence of protonic acid sites and hydride determined the activity of WO₃-ZrO₂.

Keywords; WO₃-ZrO₂, C5-C7 linear alkanes, isomerization, Bronsted acid sites, Lewis acid sites

Abstrak

Kesan WO₃ ke atas sifat dan pengisomeran-mungkin C5-C7 alkana lurus pada ZrO₂ dikaji dibawah atmosfera helium. WO₃-ZrO₂ dihasilkan dengan cara pengisitepuan Zr(OH)₄ dengan larutan aquos (NH₄)₆[H₂W₁₂O₄₀], dilanjutkan dengan pengkalsinan pada 1093 K selama 3 jam dalam udara. Jumlah WO₃ adalah 10 wt%. Pencirian XRD dan BET menunjukkan bahawa penambahan WO₃ menstabilkan fasa tetragon ZrO₂, yang meyebabkan kepada luas permukaan yang lebih besar dan keasidan lebih kukuh pada ZrO₂. Kajian Pyridine FTIR menunjukkan interaksi WO₃ dengan ZrO₂ yang membentuk tapak Lewis dan Bronsted asid yang kukuh. Kehadiran WO₃ meningkatkan pengisomeran-mungkin C5-C7 alkana lurus. Penukaran C5, C6 dan C7 mencapai 1.3, 2.6 dan 5.1 %. Dan keterpilihan

isopentana, isohexana dan isoheptana mencapai 15.6, 20.5 dan 19.5 %. Aktiviti tinggi $\text{WO}_3\text{-ZrO}_2$ adalah disebabkan oleh keupayaan WO_3 untuk menyerap dan memisahkan alkana lurus dan membentuk hidrogen dan alkana radikal di mana hidrogen atom akan menjadi tapak proton asid dan hidrida. Tahap keaktifan $\text{WO}_3\text{-ZrO}_2$ adalah ditentukan dengan kewujudan tapak proton asid dan hidrida.

Kata kunci: $\text{WO}_3\text{-ZrO}_2$, C5-C7 alkana lurus, isomeran, tapak asid Bronsted, tapak asid Lewis

© 2015 Penerbit UTM Press. All rights reserved

1.0 INTRODUCTION

In last two decades, the increasing environmental awareness has led to strong restrictions on gasoline contents in aromatic compounds, sulphur and lead. This has caused oil refineries to start and to continuously reformulate their gasoline composition in an attempt to keep their product quality while minimize adverse effects to human and environment. As a result, in regards to the RON of the gasoline, there is a need to maintain the number of available octane, which has recently attracted much interest in isomerization process involving alkanes, particularly lower linear chain alkanes such as *n*-pentane, *n*-heptane and *n*-heptane. Many studies showed that the transition metal or noble metal loaded on metal oxide¹⁻³, mesoporous^{4,5} or microporous^{6,7} materials possesses high activity for the isomerization of lower linear alkanes. Among those supports, zirconia (ZrO_2) provides an effective choice for the isomerization process owing to their relatively large surface area, large pore size, high thermal stability, easy to be modified and resistance towards coke formation.

The properties of ZrO_2 can be improved by admixtures of oxo-anions of p and d elements such as sulfate, molybdate, chromate and tungstate.⁸⁻¹² They do not form bulk solutions with ZrO_2 , but they modify the surface properties of ZrO_2 in terms of thermal stability, crystallinity, surface area, pore size distribution and acidity of ZrO_2 . In recent years, $\text{SO}_4^{2-}\text{-ZrO}_2$, $\text{MoO}_3\text{-ZrO}_2$, $\text{Cr}_2\text{O}_3\text{-ZrO}_2$ and $\text{WO}_3\text{-ZrO}_2$ have been widely explored in acid catalytic reactions such as alkane isomerization and cracking.

Recently, several research groups have extensively focused on the exploration of $\text{WO}_3\text{-ZrO}_2$, as they are more thermally and chemically stable catalyst compared to $\text{SO}_4^{2-}\text{-ZrO}_2$, $\text{MoO}_3\text{-ZrO}_2$ and $\text{Cr}_2\text{O}_3\text{-ZrO}_2$. $\text{WO}_3\text{-ZrO}_2$ can be operated at relatively high temperatures with higher selectivity and fewer cracking products without suffering from tungsten loss during reaction and undergo significantly less deactivation during the reaction.⁹ Scheithauer et al. have reported that Brønsted acid site strength on ZrO_2 depend on the WO_3 loading in which a higher WO_3 loading resulted in a higher concentration of permanent Brønsted acid sites leading to high activity of catalyst.¹³ Similarly, Naito et al. have suggested that

the permanent Brønsted acid sites on monolayer-dispersed WO_3 are active for the isomerization of *n*-butane.¹⁴ They have concluded that the maximum activity at 6.4 W atoms/nm² is in good agreement with the maximum Brønsted acidity of the catalyst. Further WO_3 loading diminishes the activity of both Lewis and Brønsted acid sites. While, Soutlanidis et al. has explored the effect of tungsten surface density in the properties and catalytic activity of *n*-pentane isomerization.¹⁰ They concluded that the surface Brønsted acidity of WZrOH sample treated at 973 K was constant at ~0.035 sites/W atom below monolayer dispersed W atom and the acidity decreased gradually above monolayer dispersed W atom. However the activity of WZrOH samples demonstrated a volcano-shape dependence on tungsten surface density with maximum activity at 5.2 W/nm² due to the large population of ZrWO_x clusters. We also have reported the influence of WO_3 loading on the properties and ability of ZrO_2 to form active protonic acid sites from molecular hydrogen.⁹ FTIR and *n*-butane isomerization suggested that 13 wt% WO_3 loading on ZrO_2 yields the highest amount of isobutene due to the presence of strong Lewis acid sites on monolayer-dispersed WO_3 facilitates the formation of protonic acid sites from hydrogen in the gas phase which act as active sites in *n*-butane isomerization. In addition we also concluded that the permanent Brønsted acid sites could not be directly associated with activity of ZrO_2 .

Although, large efforts have been undertaken to find an appropriate catalyst and an effective process for the catalytic conversion of low linear alkanes to more valuable hydrocarbon, fundamental study on the ability of catalyst to form active sites is still an interesting subject for developing new type of catalyst. In this study, we have prepared 10 wt% WO_3 loaded on ZrO_2 by impregnation method for low linear alkanes (C5, C6 and C7) isomerization under helium atmosphere at 623 K. The addition of 10 wt% WO_3 on ZrO_2 will form a strong interaction between WO_3 and ZrO_2 support which lead to form a strong acidity of catalyst. The activity of the catalyst was evaluated based on the properties of catalyst and the ability of $\text{WO}_3\text{-ZrO}_2$ to form active protonic active sites from C5, C6 and C7 linear alkanes.

2.0 EXPERIMENTAL

2.1 Preparation Of Catalyst

Zirconium hydroxide ($Zr(OH)_4$) was prepared from an aqueous solution of $ZrOCl_2 \cdot 8H_2O$ (99.9%, Wako Pure Chemical) by hydrolysis with 2.8 wt% NH_4OH aqueous solution at 353 K.¹⁵ The final pH value of the supernatant was 9.0. The precipitate was aging at 353 K for 3 h followed by aging at room temperature overnight. Then the product was filtered and washed with double deionized water till the final pH value of the supernatant was 7.0. Then the gel obtained was dried at 383 K to form $Zr(OH)_4$. The WO_3 - ZrO_2 sample was prepared by impregnation of $Zr(OH)_4$ with an aqueous $(NH_4)_6[H_2W_{12}O_{40}]$ (99.9%, Wako Pure Chemical), followed by calcination at 1093 K for 3 h in air. The amount WO_3 was 10 wt%.

2.2 Characterization Of Catalyst

The crystalline structure of catalysts was determined with XRD recorded on a Bruker AXS D8 Automatic Powder Diffractometer using Cu K α radiation with $\lambda = 1.5418 \text{ \AA}$ at 40 kV and 40 mA, over the range of $2\theta = 20\text{--}40^\circ$. The fraction of tetragonal and monoclinic phases of ZrO_2 in the catalyst was determined based on Toraya formula.¹⁶ The BET specific surface area and BJH pore size distribution of the catalyst were determined with a Beckman Coulter 3100SA at 77 K. Prior to the analysis, the catalyst was outgassed at 573 K for 3 h. Temperature-programmed desorption of ammonia (NH_3 -TPD) was carried out with ThermoQuest TPD1100 by a procedure similar to that described in previous report.¹⁵ In brief, the catalyst was activated with oxygen for 1 h at 673 K for 1 h and hydrogen flow at 673 K for 3 h followed by purging with helium flow at 673 K for 30 min, to ensure the removal of adsorbed water and organic contaminants. Then, the activated catalyst was exposed to 1.3 kPa of dehydrated ammonia at 373 K for 30 min followed by purging with helium flow at 373 K for 30 min to remove the physical adsorption of ammonia. The TPD was run at a heating rate of 10 K/min from room temperature to 900 K under the helium flow, and the desorbed ammonia was detected by mass spectrometry.

In the measurement of IR spectra, a self-supported wafer placed in an *in situ* stainless steel IR cell with CaF_2 windows was activated with oxygen flow at 623 K for 30 min and hydrogen flow at 623 K for 3 h, followed by outgassing at 623 K for 1 h.^{17,18} The sample was exposed to 0.13 kPa of pyridine at 423 K, followed by outgassing at 573 K to remove gas phase or physical adsorption of pyridine on the catalyst surface. In the alkane-exposure process, the sample pretreated at 623 K was exposed to 0.13 kPa of pyridine at 423 K for 15 min, followed by outgassing at 623 K for 15 min. Then the sample was exposed to 20 kPa of alkane (C5, C6 or C7 linear alkane) at room temperature. The sample was heated stepwise from room temperature in 50 K increments. All spectra were recorded on an Agilent Carry 640 IR spectrometer at

room temperature.

2.3 Reaction Procedure

Isomerization of C5, C6 or C7 linear alkane was carried out employing a microcatalytic pulse reactor according to the method described in the literatures.⁴ Catalyst sample of 0.2 g set in the reactor was pretreated with flowing oxygen at 673 K for 1 h and flowing hydrogen at 673 K for 3 h, followed by a flowing helium at 623 K for 1 h. A dose of C5, C6 or C7 linear alkane (43 μmol) was passed over the activated catalyst in a carrier helium flowing at 50 mL/min, and the products were trapped at 77 K before being flash-evaporated into an online 6090N Agilent gas chromatograph equipped with HP-5 Capillary Column and FID detector. The interval between doses was kept constant at 30 min. The reaction reached steady state at pulse number three (90 min). The conversion and selectivity were calculated based on the assumption that the retention time for alkanes passing through the catalyst bed is negligibly small. Thus the rate of conversion can be calculated by multiplying of conversion with reaction rate constant at 623 K.

3.0 RESULTS AND DISCUSSION

Figure 1 shows the XRD patterns for ZrO_2 and WO_3 - ZrO_2 samples. Both showed similar peaks in which the peak at about $2\theta = 30^\circ$ is assigned to tetragonal phase of ZrO_2 and the peaks at about 28° and 32° to monoclinic phase of ZrO_2 . The peak ascribed to tetragonal phase of ZrO_2 was predominant on WO_3 - ZrO_2 . The introduction of WO_3 partially eliminated and broadened the peaks assigned to the monoclinic phase of ZrO_2 and intensified the peak corresponding to the tetragonal phase of ZrO_2 . The ratio of monoclinic to tetragonal phase of ZrO_2 altered from 93/17 to 19/81 showing that the addition of WO_3 inhibits the sintering of ZrO_2 crystallites and stabilizes the tetragonal phase of ZrO_2 .¹⁹ No cubic phase and bulk crystalline of ZrO_2 was observed in this samples. In fact the addition of 10 wt% WO_3 formed 87% WO_3 coverage on ZrO_2 with the WO_3 surface density of 5.9 WO_3/nm^2 (Table 1).

The stabilization effect of tungstate in the tetragonal phase of ZrO_2 is consistent with previous reports on oxo-species such as sulfate, chromate, molybdate supported on ZrO_2 .⁸⁻¹² In addition, the effect of WO_3 on ZrO_2 has been reported by several research groups. Scheithauer et al. reported that the monoclinic phase of ZrO_2 dominated at low WO_3 content and was lower when the catalyst was calcined at 1098 K.¹⁹ An increase in WO_3 loading up to 19 wt% WO_3 increased the fraction of the tetragonal phase of ZrO_2 . Vaudagna et al. reported that bulk crystalline WO_3 was formed by calcination of the catalysts at 1103 K regardless of the degree of WO_3 loading²⁰, while Scheithauer et al. concluded that crystalline WO_3 was formed only for 19 wt% WO_3 loading on ZrO_2 with calcination temperatures of 1023

K and above.¹⁹ We have also reported the effect of WO_3 the properties of ZrO_2 in which the specific surface area and total pore volume passed through a maximum of WO_3 loading at 13 wt%; this loading corresponds to $5.9 \text{ WO}_3/\text{nm}^2$ and is near the theoretical monolayer-dispersed limit of WO_3 on ZrO_2 .⁹

Nitrogen physisorption showed that the introduction of WO_3 on ZrO_2 increases the BET specific surface area and total pore volume by about 96% and 196%, respectively (Table 1). Figure 2 shows the BJH pore size distribution of the catalysts where ZrO_2 has smaller number of pores size centered at pore diameter of 7.8 nm. The presence of WO_3 markedly increased the number of pore in the range of 4-10 nm in diameter in which this change may be related to the altering of monoclinic to tetragonal phase of ZrO_2 . In fact the specific surface area of bare WO_3 was about $3 \text{ m}^2/\text{g}$. Increase in the number of pore led to increase the BET specific surface area and total pore volume.

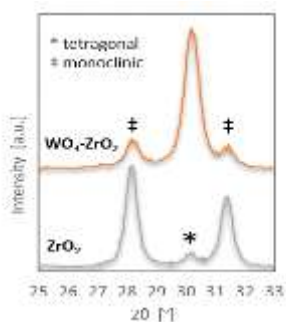


Figure 1 XRD patterns of ZrO_2 and $\text{WO}_3\text{-ZrO}_2$

Table 1 The properties of ZrO_2 and $\text{WO}_3\text{-ZrO}_2$

Terms	ZrO_2	$\text{WO}_3\text{-ZrO}_2$
WO_3 content [wt%]	-	10
BET surface area [m^2/g]	25	49
Total pore volume [mL/g]	0.029	0.086
Surface density [WO_3/nm^2]	-	5.9
WO_3 coverage [%]	-	87
Monoclinic/Tetragonal [vol%/vol%]	93/17	19/81

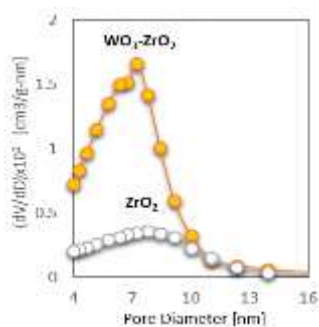


Figure 2 BJH pore size distribution of ZrO_2 and $\text{WO}_3\text{-ZrO}_2$

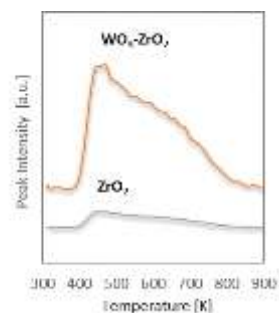


Figure 3 Ammonia TPD plots of ZrO_2 and $\text{WO}_3\text{-ZrO}_2$

Acid site distribution and strength for $\text{WO}_3\text{-ZrO}_2$ catalysts were studied by ammonia TPD and pyridine adsorbed IR spectroscopy (Figure 3 and 4). Figure 3 shows ammonia TPD plots for ZrO_2 and $\text{WO}_3\text{-ZrO}_2$. The TPD plots for $\text{WO}_3\text{-ZrO}_2$ consisted of two peaks: one main peak appearing at about 460 K and the shoulder peak at about 650 K. The shoulder peak which emerged when the catalysts were heated to 900 K reveals that the surface acid strength was widely distributed on the catalysts. While ZrO_2 possessed small single peak at 460 K and almost no-peak was observed at 500 K and above. These results indicated that ZrO_2 has almost no-acidity at all temperature experiments. Contrarily, $\text{WO}_3\text{-ZrO}_2$ possessed wide distribution of acid sites ranging from low to relatively strong acid sites in which the ammonium probe molecule desorbed at 850 K and below.

Figure 4 shows the IR spectra of pyridine adsorbed on ZrO_2 and $\text{WO}_3\text{-ZrO}_2$ to distinguish the type acidic sites. The IR bands at 1540 and 1450 cm^{-1} assigned to pyridinium ions adsorbed on Brønsted acid sites and pyridine coordinated to Lewis acid sites appeared for both catalysts, respectively. The bare ZrO_2 possessed strong Lewis acid sites at 1445 cm^{-1} due to the presence of cus Zr^{4+} , while the broad band in the range of $1515\text{--}1570 \text{ cm}^{-1}$ may be an artifact produced during preparation of the sample.¹¹ The introduction of WO_3 altered the acidity of the catalyst significantly. Particularly, the Brønsted acid sites was observed clearly at 1540 cm^{-1} and the peak assigned to Lewis acid sites shifted from 1445 to 1450 cm^{-1} . The shift of the peak must be due to the interaction of WO_3 with cus Zr^{4+} through O atom. The formation of the Brønsted acid sites due to the presence of WO_3 was also observed in the altering of the peak at 1490 cm^{-1} attributed to the combination of Lewis and Brønsted acid sites. Only small peak corresponds to Lewis acid sites at 1490 cm^{-1} was observed on bare ZrO_2 , however the peak obviously intensified with the presence of WO_3 indicating that interaction between WO_3 and ZrO_2 surface formed acidic hydroxyl groups on the surface catalyst.

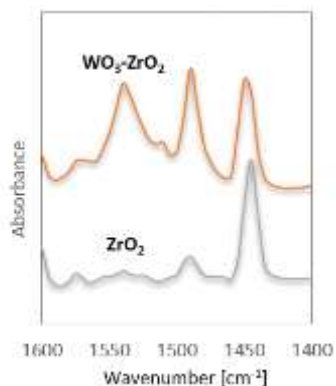
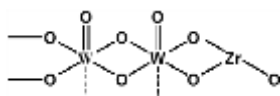


Figure 4 IR spectra of ZrO₂ and WO₃-ZrO₂ catalysts

Based on our previous IR assignment, WO₃-ZrO₂ possessed two IR bands in the W=O stretching region indicates two different types of W=O species are on the surface.²¹ The IR band at 1021 cm⁻¹ is assigned to the stretching of the W=O which is connected to *cis* Zr⁴⁺ through O. The band at 1014 cm⁻¹ is assignable to the stretching of the W=O which is connected to the other W through O. No-dioxo (O=W=O) tungsten oxide species were present in the sample, due to the different relative intensities and wavenumbers of those two bands (symmetric and antisymmetric stretching modes of the O=W=O) is less than 30 cm⁻¹. Scheme shows the proposed model and structure of WO₃-ZrO₂.



Scheme 1 Proposed model and structure of WO₃-ZrO₂.²¹

Figure 5 shows the isomerization of C₅, C₆ and C₇ linear alkanes over ZrO₂ and WO₃-ZrO₂ under helium atmosphere at 623 K in a microcatalytic pulse reactor. In general, the outlet was composed of isoproduct, C₁-C₃ cracking-products and unreacted linear alkanes. The absence of hydrogen in this experiment markedly suppressed the yield of the reaction for both ZrO₂ and WO₃-ZrO₂ due to the inability of catalysts to form active protonic acid sites and also hydride from molecular hydrogen. In addition, the catalytic activity was very low for ZrO₂ due to the absence of WO₃ which act as active specific sites in the adsorption and dissociation of linear alkanes and low concentration of permanent Brønsted acid sites. In fact the selectivity and conversion of C₅, C₆ and C₇ linear alkanes did not typically exceed than 1 %. This result clarified that the presence of active specific sites such as molecular hydrogen and also metal site such as WO₃ are indispensable in the isomerization of C₅, C₆ and C₇ linear alkanes. The addition of WO₃ on ZrO₂ altered the activity of catalyst in which the conversion of C₅, C₆ and C₇ linear alkanes reached 1.3, 2.6 and 5.1%, respectively. While the selectivity of isoproducts reached 15.6, 20.5 and 19.5 % for isopentane, isohexane and isoheptane, respectively. The increase in the activity of WO₃-ZrO₂ due to the presence of WO₃

which act as active site in the adsorption and dissociation of linear alkanes to form hydrogen and alkane radical.²² Then the hydrogen spillover into the surface of ZrO₂ and finally formed an active protonic acid sites by releasing an electron to the adjacent Lewis acid sites. The WO₃-ZrO₂ also showed good stability at 623 K, in which the activity did not decreased after 3 h of reaction. Small deactivation after 3 h may be due to the formation of coke-deposits on catalyst. In addition, both ZrO₂ and WO₃-ZrO₂ did not active for isomerization of C₅, C₆ and C₇ linear alkanes at 523 K and below. This may be due to the inability of WO₃ to adsorb and to dissociate linear alkanes to form hydrogen and alkane radical at relatively lower temperature (at and below 523 K).

We have reported the acid catalytic activity of WO₃-ZrO₂ in the isomerization of *n*-butane at 573 K in a closed recirculation batch reactor with a mixture of H₂ (40 kPa) or N₂ (40 kPa) and *n*-butane (6.67 kPa).⁹ In the presence of hydrogen gas, the product consisted of only isobutane and residual *n*-butane. It is interesting to note that neither lower nor higher linear alkanes were observed, indicating that dimerization, hydrogenolysis or cracking did not take place over WO₃-ZrO₂ in the temperature range of reaction. In addition, it has also been concluded that the activity of WO₃-ZrO₂ in *n*-butane isomerization was strongly determined by the amount of WO₃ loading. Increasing WO₃ loading improved the yield of isobutane and reached a maximum for 13wt% WO₃ loaded on ZrO₂.

Figure 6 shows the changes of IR spectrum in the region 1600-1400 cm⁻¹ when the pyridine-adsorbed WO₃-ZrO₂ was heated in the presence of A) *n*-pentane, B) *n*-hexane and C) *n*-heptane vapour up to 473 K. The peak at 1450 cm⁻¹ is ascribed to pyridine adsorbed on Lewis acid sites, and the peak at 1540 cm⁻¹ is ascribed to pyridine adsorbed on protonic acid sites as pyridinium ions. Figure 6A shows the spectra when pyridine-adsorbed WO₃-ZrO₂ was heated from 298 to 473 K in *n*-pentane vapour. As the temperature was raised, the intensity of the peak at 1450 cm⁻¹ decreased, with concomitant increased in the intensity of the peak at 1540 cm⁻¹. These results indicated that Lewis acid sites converted into protonic acid sites when the sample was heated in *n*-pentane vapour. Similar results were observed when WO₃-ZrO₂ was heated in the presence of *n*-hexane or *n*-heptane (Figure 6B-C), the intensity of Lewis acid sites decreased in tandem with the increase in the intensity of protonic acid sites. Contrarily, heating of ZrO₂ catalyst in the presence of *n*-pentane, *n*-hexane or *n*-heptane did not show any changes in the Lewis and protonic acid sites indicating there is no interchange between Lewis and protonic acid sites by contacting with linear alkanes.

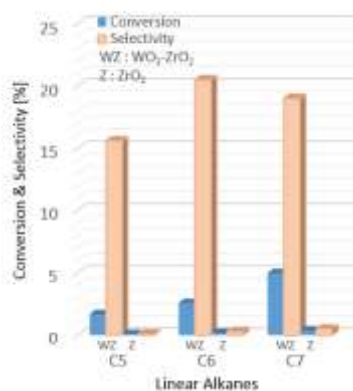


Figure 5 Isomerization of C5-C7 linear alkanes over ZrO_2 and WO_3-ZrO_2 under helium atmosphere at 623 K.

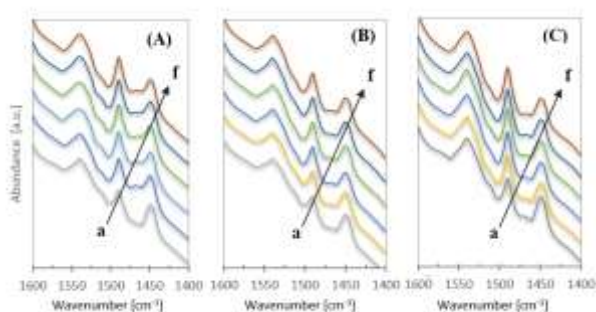


Figure 6 IR spectra of pyridine adsorbed on WO_3-ZrO_2 by heating in the presence of A) *n*-pentane B) *n*-hexane and C) *n*-heptane at different temperatures, (a) before exposure, (b) 298K, (c) 323K, (d) 373K, (e) 423K and (f) 473K.

These results clarified the ability of WO_3-ZrO_2 to isomerize low linear alkanes under helium atmosphere in which the protonic acid sites and hydride from linear alkane involve as active sites in the reaction.

Similar phenomenon was observed on $Pt/SO_4^{2-}-ZrO_2$ and $Zn/H-ZSM5$ in which the generation of protonic acid sites from *n*-pentane molecules was observed by IR study of adsorbed pyridine over the surfaces of $Pt/SO_4^{2-}-ZrO_2$ and $Zn/H-ZSM5$ at temperature range of 300–600 K.²² It is postulated that the protonic acid sites are generated through dissociation of pentane molecules to hydrogen atoms and pentyl radicals followed by spillover of the hydrogen atoms onto the support and migration to reach Lewis acid site where the hydrogen atoms donates electrons to Lewis acid site and becomes protonic acid sites. Although the catalytic activity was not reported in detail, the changing of the Lewis to become protonic acid sites over $Pt/SO_4^{2-}-ZrO_2$ and $Zn/H-ZSM5$ by contact with *n*-pentane vapour promising the possibility of catalyst to be used for a number of acid-catalyzed reaction. It should be noted that the formation of protonic acid sites an *n*-pentane radical over $Pt/SO_4^{2-}-ZrO_2$ and $Zn/H-ZSM5$ is a reversible process in which heating in the vacuum restored the Lewis acid sites to almost its original concentration and eliminated the formed protonic acid sites.

4.0 CONCLUSION

The generation of protonic acid sites from *n*-pentane, *n*-hexane and *n*-heptane molecules was observed by IR study of adsorbed pyridine over the surfaces of WO_3-ZrO_2 . The protonic acid sites are generated through dissociation of alkane molecules to form hydrogen atoms and alkane radicals followed by spillover of the hydrogen atoms onto the support and migration to reach Lewis acid site where the hydrogen atoms donates electrons to adjacent Lewis acid site and becomes protonic acid sites. The other hydrogen atoms may interact with electrons to form hydrides on the catalyst surface. Then the formed protonic acid sites and hydrides involved in the isomerization to form isoproducts with the selective range of 15–20 %. While the conversion of C5, C6 and C7 linear alkanes did not exceed 5 %. This result suggested the protonic acid sites formed from the reactant over WO_3-ZrO_2 is able isomerize the reactant itself, however they did not satisfy to improve the catalytic isomerization of C5, C6 and C7 linear alkanes significantly.

Acknowledgement

The author would like to thank the Ministry of Higher Education (MOHE), Malaysia through the Fundamental Research Grant Scheme No. 4F161. Our gratitude also goes to the Hitachi Scholarship Foundation for the Gas Chromatograph Instruments Grant.

References

- [1] Sugeng Triwahyono, Aishah A. J., S. Najjha T., N. N. Ruslan, H. Hattori. 2010. Kinetics Study of Hydrogen Adsorption on Pt/MoO_3 . *Applied Catalysis A: General*. 372: 103-107.
- [2] U. B. Demirci, F. Garin 2007. Kinetic study of *n*-heptane conversion on palladium or iridium supported on sulphated zirconia. *Journal of Molecular Catalysis A: Chemical*. 271:216-220
- [3] H. Al-Kandari, F. Al-Kharafi, A. Katrib. 2009. Large scale hydroisomerization reactions of *n*-heptane on partially reduced MoO_3/TiO_2 . *Applied Catalysis A: General*. 361:81–85
- [4] S. Triwahyono, A. A. Jalil, N. N. Ruslan, H. D. Setiabudi, N.H.N. Kamarudin. 2013. C5-C7 linear alkane hydroisomerization over MoO_3-ZrO_2 and Pt/MoO_3-ZrO_2 catalysts. *Journal of Catalysis*. 303:50–59.
- [5] N. H. R. Annuar, S. Triwahyono, A. A. Jalil, N. A. A. Fatah, L. P. Teh, C.R. Mamat. 2014. Effect of chromium precursor on the properties of chromium oxide zirconia. *Applied Catalysis A: General*. 475: 487-496.
- [6] H. D. Setiabudi, A. A. Jalil, S. Triwahyono. 2012. Ir/ $Pt-HZSM5$ for *n*-pentane isomerization: Effect of iridium loading on the properties and catalytic activity. *Journal of Catalysis*. 294: 128-135.
- [7] A. Christodoulakis, S. Boghosian. 2008. Molecular structure and activity of molybdena catalysts supported on zirconia for ethane oxidative dehydrogenation studied by operando Raman spectroscopy. *Journal of Catalysis* 260: 178–187
- [8] B. Samaranch, P. R. Piscina, G. Clet, M. Houalla, N. Homs, 2006. Study of the Structure, Acidic, and Catalytic Properties of Binary Mixed-Oxide MoO_3-ZrO_2 Systems.

- Chemistry of Material*. 18: 1581–1586
- [9] A. H. Karim, Sugeng Triwahyono, Aishah Abdul Jalil, Hideshi Hattori. 2012. WO₃ monolayer loaded on ZrO₂: Property-activity relationship in n-butane isomerization evidenced by hydrogen adsorption and IR studies. *Applied Catalysis A: General*. 433-434:49-57.
- [10] N. Soutanidis, W. Zhou, A. C. Psarras, A. J. Gonzalez, E. F. Iliopoulou, C. J. Kiely, I. E. Wachs, M. S. Wong. 2010. Relating n-Pentane Isomerization Activity to the Tungsten Surface Density of WO_x/ZrO₂. *Journal of American Chemical Society*. 132:13462–13471.
- [11] N. N. Ruslan, N. A. Fadzillah, A.H. Karim, A.A. Jalil, S. Triwahyono. 2011. IR study of active sites for n-heptane isomerization over MoO₃-ZrO₂. *Applied Catalysis A: General*. 406: 102-112.
- [12] Muhammad Arif Ab Aziz, Nur Hidayatul Nazirah Kamarudin, Herma Dina Setiabudi, Halimatun Hamdan, Aishah Abdul Jalil, Sugeng Triwahyono. 2012. Negative effect of Ni on PtHY in n-pentane isomerization evidenced by IR and ESR studies. *Journal of Natural Gas Chemistry*. 21: 29-36
- [13] M. Scheithauer, T.-K. Cheung, R. E. Jentoff, R.K. Grasselli, B.C. Gates, H. Knozinger. 1998. Characterization of WO_x/ZrO₂ by vibrational spectroscopy and n-pentane isomerization catalysis. *Journal of Catalysis*. 180: 1–13.
- [14] N. Naito, N. Katada, M. Niwa. 1999. Tungsten oxide monolayer loaded on zirconia: Determination of acidity generated on the monolayer. *Journal of Physical Chemistry B*. 103: 7206–7213.
- [15] Sugeng Triwahyono, T. Yamada, H. Hattori. 2003. Effects of Na Addition, Pyridine, and Water on Hydrogen Adsorption Property of Pt/SO₄²⁻-ZrO₂. *Catalysis Letter*. 85: 109-115.
- [16] H. Toraya, S. Yoshimura, S. Somiya. 1984. Calibration curve for quantitative analysis of the monoclinic-tetragonal ZrO₂ system by X-Ray diffraction. *Journal of American Ceramic Society*. 67: 119–121.
- [17] Sugeng Triwahyono, Zalizawati Abdullah, Aishah Abdul Jalil. 2006. The Effect of Sulfate Ion on the Isomerization of n-Butane to iso-Butane. *Journal of Natural Gas Chemistry*. 15: 247-252
- [18] Herma Dina Setiabudi, Aishah Abdul Jalil, Sugeng Triwahyono, Nur Hidayatul Nazirah Kamarudin, Rino R. Mukti. 2012. IR study of iridium bonded to perturbed silanol groups of Pt-HZSM5 for n-pentane isomerization. *Applied Catalysis A: General*. 417–418: 190–199
- [19] M. Scheithauer, R. K. Grasselli, H. Knozinger. 1998. Genesis and structure of WO_x/ZrO₂. *Langmuir*. 14: 3019–3029.
- [20] S. R. Vaudagna, S. A. Canavese, R. A. Comelli, N. S. Figoli. 1998. Platinum supported WO_x-ZrO₂: Effect of calcination temperature and tungsten loading. *Applied Catalysis A: General*. 168: 93–111.
- [21] Sugeng Triwahyono, Takashi Yamada, Hideshi Hattori. 2003. IR study of acid sites on WO₃-ZrO₂. *Applied Catalysis A: General*. 250: 75–81
- [22] Sugeng Triwahyono, Aishah A. J., Malik M. 2010. Generation of protonic acid sites from pentane on the surface of Pt/SO₄²⁻-ZrO₂ and Zn/HZSM5 evidenced by IR study of adsorbed pyridine. *Applied Catalysis A: General*. 372: 90-193
- .